Pergamon

Geochimica et Cosmochimica Acta, Vol. 59, No. 18, pp. 3871–3875, 1995

0016-7037/95 $9.50 + .00

0016-7037(95)00309-6

LETTER

Determination of the magnetite-water equilibrium oxygen isotope fractionation factor at 350°C: A comparison of ion microprobe and laser fluorination techniques

STEVEN M. FORTIER,[1] DAVID R. COLE,[1] DAVID J. WESOLOWSKI,[1] LEE R. RICIPUTI,[1]
BRUCE A. PATERSON,[1] JOHN W. VALLEY,[2] and JUSKE HORITA[1]

[1]Chemical and Analytical Sciences Division, Oak Ridge National Laboratory, Oak Ridge, TN 37831-6110, USA
[2]Department of Geology and Geophysics, University of Wisconsin, Madison, WI 53706, USA

(*Received June* 12, 1995; *accepted in revised form August* 8, 1995)

Abstract—A Cameca 4f ion microprobe has been used in conjunction with laser and conventional analytical techniques to measure the oxygen isotope fractionation between magnetite and water at 350°C. A set of experiments in which large (10–200 μm) magnetite crystals were grown from fine grained (0.2–2 μm) hematite starting material using four different isotopically labelled waters yields a value of 1000 ln $\alpha_{(mt\text{-}w)} = -8.47 \pm 0.23$, as determined by bulk oxygen extraction using laser fluorination. The value from the ion microprobe determination based on replicate analysis of magnetite single crystals is -8.60 ± 0.65. The bulk analysis of one of the set of four experiments was used as an internal ion microprobe standard. The good agreement between the two techniques suggests that ion microprobe analyses may permit determination of isotope fractionation factors in experiments involving only a few percent of overall exchange.

1. INTRODUCTION

Equilibrium oxygen isotope fractionation between minerals and other phases is notoriously difficult to measure experimentally at temperatures below about 400 to 500°C. The relatively slow rates of exchange of oxygen between minerals and water commonly precludes a significant fractional approach to equilibrium. Despite this fundamental difficulty, the application of isotope geothermometry in low temperature systems such as geothermal reservoirs and sedimentary basins has prompted the development and use of various methods for calculating fractionation factors and their temperature dependence at $T < 500$°C (e.g., statistical mechanical calculations: Kieffer, 1982; Clayton and Kieffer, 1991; increment method: Schütze, 1980; Richter and Hoernes, 1988; Zheng, 1991, 1993; Hoffbauer et al., 1994).

The iron oxide minerals magnetite (Fe_3O_4) and hematite (Fe_2O_3) are particularly important accessory minerals in a wide variety of geological and industrial environments. These minerals also illustrate very clearly the enormous discrepancies that occur in the literature between various empirical, experimental, and quasi-theoretical estimates of the value of fractionation factors at low temperature. Magnetite-water fractionations at temperatures between 400 and 25°C, as estimated by various authors, differ by between 3 and 12‰, depending on the model or data employed. For example, the empirical data of Blattner et al. (1983) and the model of Clayton and Kieffer (1991) (when the latter is combined with the experimental data of O'Neil et al., 1969) differ by ≈10‰ at 100°C. Clearly, a well-controlled experimental calibration could resolve this situation.

Results from solubility (Palmer and Drummond, 1992) and kinetics experiments (Bell et al., 1994) indicate that coarse-crystalline magnetite can be grown by reductive dissolution of hematite and recrystallization in dilute acetic acid solutions at temperatures down to at least 300–335°C. By taking advantage of recent advances in ion microprobe analysis of natural samples (e.g., Valley and Graham, 1991; Riciputi and Paterson, 1994) we are now capable of measuring fractionation factors by replicate analysis of magnetite single crystals, grown using acetic acid as a "mineralizer." The ion microprobe results are compared with those obtained by bulk analysis (i.e., laser fluorination) to test the validity of the approach. The ability to determine fractionation factors from analysis of single crystals opens up the low temperature regime to experimental studies. Crystals with a cross section of a few tens of microns are sufficient for ion microprobe analysis with useful accuracy and with precision approaching that of bulk analysis techniques.

2. METHODS

2.1. Experimental

A 0.2–2.0 μm reagent grade synthetic hematite (Fig. 1a) with $\delta^{18}O = +9.62 \pm 0.04$‰ (VSMOW) (analyzed by laser fluorination) was used for all experiments. Four waters with different initial $\delta^{18}O$ were used: W1: −7.52‰; W2: +48.27‰; W3: +23.52‰; W4: −36.89‰; (all permil values for water are normalized on the VSMOW/SLAP scale with uncertainties of order 0.05‰ and were measured using CO_2-H_2O equilibration). Magnetite was synthesized at 350°C and 1 kb for 9 weeks, in 5 mm Au tubes, by recrystallization of hematite starting material in the presence of 0.5 m acetic acid. The aqueous solutions were prepared by the addition of the appropriate amounts of 100% glacial acetic acid to each starting water. The fluid to solid ratio was 20:1 by weight. The overall reaction mechanism presumably involves reductive dissolution of hematite, releasing Fe^{3+} into solution, followed by precipitation and growth of magnetite. Octahedral and dodecahedral magnetite crystals ranging in size from 10 to more than 200 μm were readily grown in this way with nearly complete consumption of the hematite starting material. Conversion to magnetite was verified by XRD and SEM. Further details of the

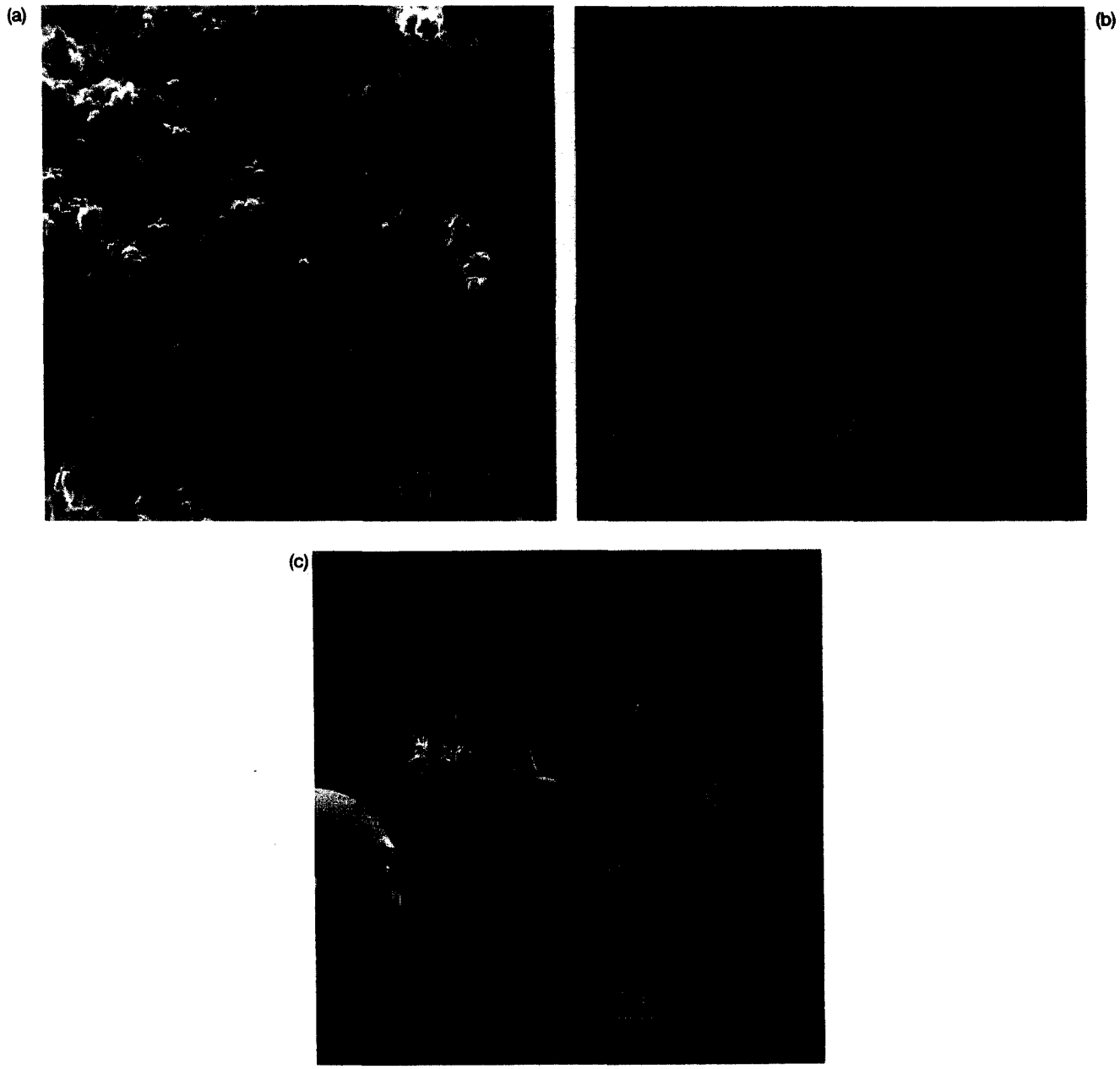

FIG. 1. (a) SEM photo of fine grained, synthetic hematite starting material. (b) SEM photo of coarse grained, well crystallized, magnetite run products. (c) SEM photo of a magnetite grain showing four spots that were analyzed with the ion microprobe. The large grain size allows multiple ≈30 μm spot analyses on a single crystal. Areas where the surface of the grain are not well polished are clearly visible and thus easily avoided.

rates and mechanism of this reaction will be presented elsewhere. For the purposes of this paper, it is sufficient to observe that relatively large crystals can be produced (Fig. 1b) which then allow isotope ratio measurements with the ion microprobe (Fig. 1c). Since each charge consists of several hundred to a few thousand crystals, the removal of a few large single crystals for ion microprobe analysis does not significantly effect the mass balance of the system, and thus a conventional analysis can be made on the remaining sample.

2.2. Analytical

2.2.1. *Ion microprobe*

Magnetite single crystals were analyzed using a modified Cameca 4f ion microprobe using techniques detailed in Riciputi and Paterson (1994), which are only summarized here. Grains were mounted in 2.54 cm diameter epoxy plugs, polished, and coated with a thin (<0.1 μm) layer of gold to ensure surface conductivity. The samples were sputtered using a 4–6 nA primary beam of $^{133}Cs^+$ ions with total energy of 14.15 keV, focused to a beam diameter of 25–30 μm (Fig. 1c). Negative secondary ions (1.4×10^6 cps on ^{16}O) were extracted using extreme energy filtering (350 eV offset relative to the peak intensity) to eliminate hydride interferences and to minimize surface effects on instrumental mass bias. Each analysis consisted of 200 individual ratios (1 s on ^{16}O, 5 sec on ^{18}O), took 27 min, and has an internal precision of ±0.65‰ (1σ).

2.2.2. *Laser fluorination*

Bulk hematite and magnetite powders were analyzed by laser fluorination at the University of Wisconsin. Details of this system and

analytical procedures are documented in Kohn et al. (1993). Samples were pretreated overnight in the sample chamber with ≈1000 μmol BrF_5 to remove H_2O and traces of organic compounds. A 32 W CO_2 laser with a defocused laser beam ≈500 μm in diameter was used to heat samples in the presence of ≈1000 μmol of BrF_5. Typically, 2–2.5 mg size samples were reacted for 1–2 minutes. An interlaboratory standard (UW Gore Mountain garnet #2; Valley et al., 1995) was analyzed before and after analysis of the oxides to evaluate any oxygen isotope fractionation in the extraction system. The value of the standard was 5.72 ± 0.04‰ $n = 7$ and no correction was needed for the magnetite samples reported here, which are reported in the standard permil notation relative to VSMOW.

3. RESULTS AND DISCUSSION

The results of laser fluorination, bulk oxygen extraction are given in Table 1 and are plotted in Fig. 2. Information required for the mass balance calculations is included as well. The mole fraction of oxygen contained in the solution, for example, increases during the course of the experiment since oxygen is liberated by the conversion of hematite to magnetite. This information is necessary to calculate the shift in the oxygen isotope composition of the water, which changes significantly (0.14–0.87‰), despite the fact that it dominates the oxygen budget in the experiments (>98%). The calculation of the final $\delta^{18}O$ for the water was made assuming that the original hematite was converted completely to magnetite. The latter assumption, though only approximately correct, introduces uncertainties in the calculated fractionation of less than 0.01‰ and thus may safely be ignored.

The contribution of oxygen from the acetic acid is also ignored in these calculations because (1) its contribution to the total oxygen is very small (≈1.7%); (2) chemical analysis of the fluid after the run indicates that only about 20% of the acetic acid is consumed (concentration changes from 0.50 to 0.40 molal); and (3) its isotopic composition and rate of exchange with water are unknown. Unless the acetic acid oxygen isotope composition is radically different from the starting materials, it is unlikely to have a large effect. If it falls within the range of the values for the starting materials, which is likely given the size of this range, then the effects on the total $\delta^{18}O$ would be on the order of 0.1‰ or less.

Using the classical partial approach to equilibrium technique of Northrop and Clayton (1966), the value of the fractionation factor at equilibrium is determined from the intercept of a plot of the difference in the isotopic composition of the starting materials (1000 ln α_i) vs. the isotopic shift produced during the experiment 1000 (ln α_f − ln α_i) (Fig. 2).

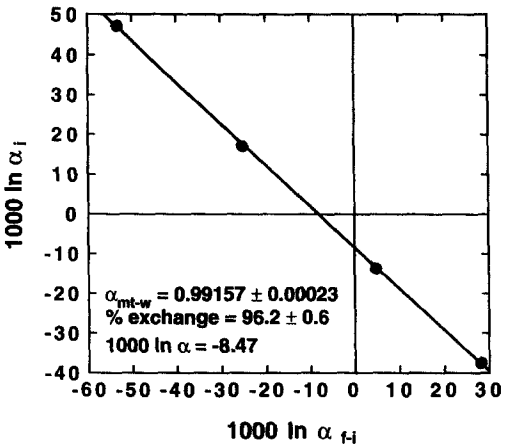

FIG. 2. Partial approach to equilibrium plot of the magnetite-water data from laser fluorination analysis, after Northrop and Clayton (1966). Plotted are the isotopic differences of the starting materials (1000 ln α_i) vs. the isotopic shift produced during the experiment (1000 ln α_{f-i}). The intercept, by definition, is the fractionation factor at equilibrium. The line is a least squares fit of the data.

The line is a least squares fit of the laser fluorination data and is linear (r^2 = 0.99990) yielding an intercept that is well constrained (−8.47 ± 0.23). It should be noted here that this value falls in the middle of the range of values predicted by the various models referred to above. The isotopic exchange is nearly, but not quite, complete (96.2 ± 0.6%), a point that is discussed further below.

Knowing the value of the fractionation factor, we can assess the degree to which the conventional and ion microprobe data agree (Table 2). The raw ion probe analyses represent 200 cycles of $^{18}O/^{16}O$ measurements at individual spots on one or more single grains as indicated in Table 2, converted to δ notation relative to VSMOW. Small magnetite grains, 20–40 μm in diameter, were probed only once, whereas larger grains could be analyzed several times, depending on their size. For example, four spot analyses were made on one crystal and a single analysis on a second crystal from experiment H1. Although there are exceptions, the reproducibility of both intra- and inter-crystalline spot analyses is better than 1‰, suggesting isotopic homogeneity of the run products.

The sputtering, ion extraction, transmission, and detection processes in the ion microprobe cause relatively large mass bias in the measured isotopic ratio which is mineral specific and must be corrected for by using appropriate standards. The

Table 1. Results from laser fluorination bulk analysis of iron oxides and CO_2 equilibration with H_2O

Exp. #	$\delta^{18}O,w_i$ (‰)(1)	mol frac O, w, i(2)	$\delta^{18}O_T$ (‰)(3)	mol frac O, w, f(4)	$\delta^{18}O,mt_f$ (‰)(5)	$\delta^{18}O,w_f$ (‰)(6)	10^3 ln α_i (7)	10^3 ln α_f (8)	10^3(lnα_f - lnα_i) (9)
H1	-7.52	0.9839	-7.24	0.9892	-15.03 ±0.03	-7.15	17.12	-7.96	-25.08
H2	48.27	0.9835	47.63	0.9890	37.95 ±0.03	47.74	-37.57	-9.39	28.18
H3	23.52	0.9830	23.29	0.9887	14.51 ±0.04	23.39	-13.68	-8.71	4.96
H4	-36.89	0.9828	-36.09	0.9885	-41.80 ±0.48	-36.02	47.16	-6.01	-53.17

(1) initial $\delta^{18}O$ of water on VSMOW/SLAP scale
(2) mole fraction of total O in H_2O at start of experiment
(3) $\delta^{18}O$ of a mixture of hematite starting material (+9.62 ‰) and initial H_2O
(4) mole fraction of total O in H_2O at end of experiment
(5) $\delta^{18}O$ of magnetite run product, measured by bulk extraction of O by laser fluorination
(6) $\delta^{18}O$ of final H_2O, calculated from mass balance
(7) intial difference between hematite and H_2O starting materials
(8) final difference between magnetite and H_2O run products
(9) oxygen isotope shift produced during the course of the experiment

Table 2. Results from ion microprobe analysis of magnetite single crystals

	H1	H2	H3	H4
raw data	gr. 1: -67.52	gr. 1: -14.11	gr. 1: -36.21	gr. 1: -92.51
(‰, VSMOW)	" : -66.88	gr. 2: -12.72	" : -37.35	" : -92.21
	" : -66.88	" : -13.42	gr. 2: -37.30	" : -93.11
	" : -66.78	gr. 3: -14.56	gr. 3: -36.90	" : -91.96
	gr. 2: -65.08	" : -13.81		
		" : -13.91		
mean	-66.63	-13.76	-36.94	-92.45
corrected for	-17.52	38.75	15.47	-43.85
ion probe	-16.85	40.22	14.27	-43.53
fractionation	-16.85	39.48	14.32	-44.48
(‰, VSMOW)	-16.74	38.28	14.74	-43.27
	-14.95	39.07		
		38.96		
mean	-16.58	39.13	14.70	-43.78
equilibrium	0.98956	0.99142	0.99226	0.99188
fractionation	0.99024	0.99282	0.99109	0.99221
factors	0.99024	0.99212	0.99114	0.99122
($\alpha_{mt\text{-}w}$)	0.99034	0.99097	0.99155	0.99248
	0.99215	0.99173		
		0.99163		
mean	0.99051	0.99178	0.99151	0.99195
std. dev.	0.00097	0.00063	0.00054	0.00054
1000 ln $\alpha_{(mt\text{-}w)}$	-9.54	-8.25	-8.53	-8.08

absolute mass bias measured on the ion microprobe for a given mineral varies by a few permil over time thus calibration is required for each analytical session. For our system, the instrumental mass bias typically remains constant within analytical precision for analytical sessions lasting up to five days. The establishment of isotopically uniform standards (on the μm scale) is in its infancy and remains one of the outstanding problems for the routine, accurate analysis of natural oxygen isotope abundances by ion probe. In our case, since we have conventional analyses of the run products, we can select from one of four possible internal standards. Each of the single crystals which are at equilibrium with the fluid in which they grew should yield a separate value of the fractionation factor. Fixing the mean ion microprobe value of one of the set of four experiments to its conventional $\delta^{18}O$ value provides an internal standard that allows us to calculate the instrumental mass bias. Sample number H3 was adopted as the internal standard since its final, bulk $\delta^{18}O$ (+14.51 $\pm$ 0.04‰) is closest to that for the starting hematite (+9.62 $\pm$ 0.04‰), and both its intracrystalline and intercrystalline reproducibility are excellent. Since the oxygen isotope exchange is not complete, the bulk analysis reflects a combination of completely exchanged magnetite and presumably unexchanged hematite starting material. The latter assumption is probably reasonable since the exchange almost certainly occurs when the iron is in solution. Correcting for 3.8% of unreacted hematite yields a $\delta^{18}O$ for magnetite single crystals in experiment H3 of +14.70 $\pm$ 0.04‰. It makes no difference, in principle, which of the set of four experiments is chosen as the standard. The ion microprobe fractionation factor determined using H3 as the internal standard is 0.94911 while those using H2 and H4 are 0.94916 and 0.94915, respectively, differences of less than 0.1‰. The value obtained from H1, on the other hand, differs by about 0.5‰ owing to its relatively poor agreement with the other experiments.

The corrected conventional value for H3 single crystal magnetite can be used to correct for the instrumental mass bias for the ion microprobe data. The raw δ-values relative to VSMOW are given in the top part of Table 2. The difference between H3 single crystals and other crystals H_i, expressed as a fractionation factor, α_{H3-H_i}, can be calculated using the equation

$$\alpha_{H3-H_i} = (\delta^{18}O_{H3,i.p.} + 1000)/(\delta^{18}O_{H_i,i.p.} + 1000), \quad (1)$$

where the subscript i.p. refers to the raw δ-values from the ion probe. Next, the corrected δ-value for H3 from laser fluorination is used to calculate those for the other experiments:

$$\delta^{18}O_{H_i} = ((\delta^{18}O_{H3,corr.} + 1000)/\alpha_{H3-H_i}) - 1000. \quad (2)$$

Values of $\delta^{18}O_{H_i}$, including ones for H3 since individual spot analyses differ from the mean value used to make the ion probe fractionation correction, are included in the middle section of Table 2. These can in turn be used to calculate individual values of the equilibrium fractionation factor, $\alpha_{mt\text{-}w}$, between magnetite and the appropriate water. The latter is calculated from mass balance as described above. Values of $\alpha_{mt\text{-}w}$ are given in the bottom section of Table 2. Uncertainties (1 σ of the mean values) indicate errors on the order of 0.5 to 1‰ from replicate analysis of the different experiments with the ion microprobe, very similar to the internal precision for each single analysis (0.65‰).

The mean fractionation factors from Table 2 are plotted vs. experiment number in Fig. 3; the horizontal line represents the value determined from laser fluorination bulk analyses with the shaded box representing the uncertainty. The agreement of ion probe and the laser fluorination results for H3 is, of course, artificial since it was used to determine the instrumental fractionation. The uncertainty of H3 is relevant, however, and therefore it was included. While there is clearly scatter in the individual spot analyses (Table 2), there is also clear overall agreement between the two types of analysis. The mean of all four ion probe fractionation factors is, in fact, the same within error (−8.60 $\pm$ 0.65). Omitting H3 or calculating the mean of all nineteen individual fractionation factors does not change the value significantly.

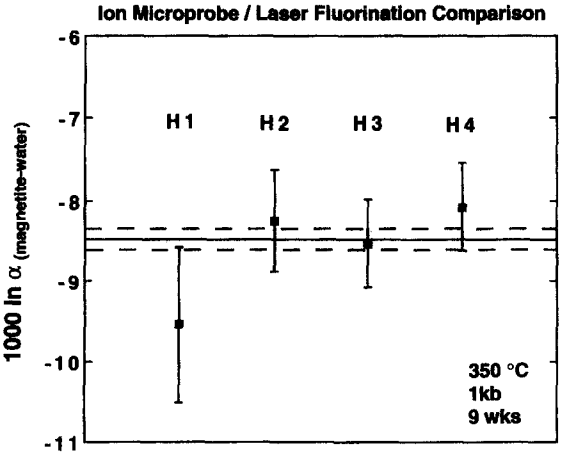

FIG. 3. Plot comparing the average values of 1000 ln $\alpha_{mt\text{-}w}$ from the ion microprobe technique for the four individual experiments (H1 through H4) with that from the laser fluorination technique (horizontal line). The shaded rectangle represents the standard error in the intercept from Fig. 2. Error bars for the individual data points are 1σ errors from Table 2.

This example demonstrates that it is possible to determine oxygen isotope fractionation factors accurately using the ion microprobe if standardized against an appropriate, homogeneous material. In this instance the fraction of isotopic exchange was high (0.962). This is not generally the case, particularly at low temperatures where much experimental work remains to be done. As percent exchange decreases, the uncertainties in the partial approach to equilibrium technique increase. This is because the slope on plots of ($1000 \ln \alpha_i$) vs. $1000 (\ln \alpha_f - \ln \alpha_i)$ steepens and thus small departures from linearity can result in relatively large uncertainties in the intercept (O'Neil, 1986) which is, by definition, the value of the fractionation factor at equilibrium. While it is not possible to prove that recrystallization or synthesis experiments represent equilibrium fractionation we have assumed that to be the case for the fractionation we have measured. Regardless of whether the measured effects are equilibrium or kinetic, however, the agreement between the two techniques stands. The ion microprobe approach provides a viable alternate method, provided crystals of adequate size (alternatively, overgrowths and/or reaction rims) can be grown.

Analytical precision is ultimately limited by counting statistics, which impose constraints on the volume of material required using this technique. A crater 30 μm in diameter and 4 μm deep, for a total sample volume of 2.8×10^3 μm^3, is required for a precision of 0.6‰ using the extreme energy offset technique of Riciputi and Paterson (1994). Increasing the spot size to 45 μm would allow an analysis with the same precision from a crater only 2 μm deep. Experiments indicate that the primary beam spot size can be reduced to 15 μm without compromising the analysis, allowing measurement of smaller grains than were used in this study. Counting statistics would then require greater crater depths. Alternatively, accepting a slightly poorer precision would reduce the required volume significantly (1‰ precision reduces the required volume by ≈66%, for example).

This technique can also be used with insulating phases, as Riciputi and Paterson (1994) have demonstrated that the same precision (≈0.6‰) can be obtained on a variety of silicate and carbonate minerals. Although the instrumental mass bias varies from mineral to mineral, and is dependent on the chemical composition within a particular mineral group, suitable standards can be identified using a combination of conventional and ion microprobe techniques. Such a capability dramatically opens up the low temperature regime to the experimentalist, which should help resolve the large uncertainties in low temperature oxygen isotope fractionations between minerals and fluids.

Acknowledgments—This study was supported by the Geosciences Program of the Office of Basic Energy Research, U.S. Department of Energy, under contract AC05-84OR21400 with Lockheed Martin Energy Systems, Inc., grant #DE-FG02-93ER 14389 to JWV, and the ORNL Laboratory Directed Research and Development Program. SMF and BAP were also sponsored by ORAU/ORISE. Helpful reviews of the manuscript were provided by I. Hutcheon and an anonymous reviewer. Thanks are due to D. Joyce (ORNL) for acetate analyses, T. Labotka (UTK) for access to the XRD facility, D. Coffey (ORNL) for excellent SEM work, N. Kitchen (UW) for stable isotope analysis by laser fluorination, and M. Gillispie (ORNL) for photography.

Editorial handling: J. D. Macdougall

REFERENCES

Bell J. L. S., Palmer D. A., Barnes H. L., and Drummond S. E. (1994) Thermal decomposition of acetate: III. Catalysis by mineral surfaces. *Geochim. Cosmochim. Acta* **58,** 4155–4177.

Blattner P., Braithwaite W. R., and Glover R. B. (1983) New evidence on magnetite oxygen isotope geothermometers at 175 and 112 C in Wairakei steam piplelines (New Zealand). *Isotope Geosci.* **1,** 195–204.

Clayton R. N. and Kieffer S. W. (1991) Oxygen isotopic thermometer calibrations. In *Stable Isotope Geochemistry: A Tribute to Samuel Epstein* (ed. H. P. Taylor Jr. et al.); *Geochim. Soc. Spec. Publ. 3,* pp. 3–10.

Elsenheimer D. and Valley J. W. (1992) In situ oxygen isotope analysis of feldspar and quartz by Nd-YAG laser microprobe. *Chem. Geol.* **101,** 21–42.

Hoffbauer R., Hoernes S., and Fiorentini E. (1994) Oxygen isotope thermometry based on a refined increment method and its application to granulite grade rocks from Sri Lanka. *Precamb. Res.* **66,** 199–220.

Kieffer S. W. (1982) Thermodynamics and lattice vibrations of minerals: 5. Applications to phase equilibria, isotope fractionation, and high pressure thermodynamic properties. *Rev. Geophys. Space Phys.* **20,** 827–849.

Kohn M. J., Valley J. W., Elsenheimer D., and Spicuzza M. (1993) Oxygen isotope zoning in garnet and staurolite: evidence for closed system mineral growth during regional metamorphism. *Amer. Mineral.* **78,** 988–1001.

Northrop D. A. and Clayton R. N. (1966) Oxygen-isotope fractionations in systems containing dolomite. *J. Geol.* **74,** 174–196.

O'Neil J. R. (1986) Theoretical and experimental aspects of isotopic Fractionation. In *Stable Isotopes in High Temperature Geological Processes* (ed. J. W. Valley et al.); *Rev. Mineral.* **16,** pp. 1–40.

O'Neil J. R., Clayton R. N., and Mayeda T. K. (1969) Oxygen isotope fractionation in divalent metal carbonates. *J. Chem. Phys.* **51,** 5547–5558.

Palmer D. A. and Drummond S. E. (1992) An experimental study of the solubility of magnetite in sodium acetate solutions. *Proc. Intl. Conf. Interact. Iron Based Mater. Water & Steam* **4-4.**

Richter R. and Hoernes S. (1988) The application of the increment method in comparison with experimentally derived and calculated O-isotope fractionations. *Chem. Erde* **48,** 1–18.

Riciputi L. R. and Paterson B. A. (1994) High spatial-resolution measurement of O isotope ratios in silicates and carbonates by ion microprobe. *Amer. Mineral.* **79,** 1227–1230.

Schütze H. (1980) Der Isotopenindex—Eine Inkrementenmethode zur näherungsweisen Berechnung von Isotopenaustauschgleichgewichten zwischen kristallen Substanzen. *Chem. Erde* **39,** 321–334.

Valley J. W. and Graham C. M. (1991) Ion microprobe analysis of oxygen isotope ratios in granulite facies magnetites: Diffusive exchange as a guide to cooling history. *Contrib. Mineral. Petrol.* **109,** 38–52.

Valley J. W., Kitchen N., Kohn M. J., Niendorff C. R., and Spicuzza M. J. (1995) UWG-2, a garnet standard for oxygen isotope ratios: Strategies for high precision and accuracy with laser heating. *Geochim. Cosmochim. Acta* (submitted).

Zheng Y.-F. (1991) Calculation of oxygen isotope fractionation in metal oxides. *Geochim. Cosmochim. Acta* **55,** 2299–2307.

Zheng Y.-F. (1993) Calculation of oxygen isotope fractionation in anhydrous silicate minerals. *Geochim. Cosmochim. Acta* **57,** 1079–1091.